Charge transfer interactions of a Ru(II) dye complex and related ligand molecules adsorbed on Au(111)

Andrew J. Britton, Matthew Weston, J. Ben Taylor, Anna Rienzo, Louise C. Mayor, and James N. O'Shea

Citation: The Journal of Chemical Physics **135**, 164702 (2011); doi: 10.1063/1.3656682
View online: http://dx.doi.org/10.1063/1.3656682
View Table of Contents: http://scitation.aip.org/content/aip/journal/jcp/135/16?ver=pdfcov
Published by the AIP Publishing

Charge transfer interactions of a Ru(II) dye complex and related ligand molecules adsorbed on Au(111)

Andrew J. Britton,[1,2] Matthew Weston,[1,2] J. Ben Taylor,[1] Anna Rienzo,[1] Louise C. Mayor,[1] and James N. O'Shea[1,2,a)]

[1]*School of Physics and Astronomy, University of Nottingham, Nottingham NG7 2RD, United Kingdom*
[2]*Nottingham Nanotechnology and Nanoscience Centre (NNNC), University of Nottingham, Nottingham NG7 2RD, United Kingdom*

(Received 24 August 2011; accepted 10 October 2011; published online 25 October 2011)

The interaction of the dye molecule, N3 (cis-bis(isothiocyanato)bis(2,2′-bipyridyl-4,4′-dicarboxylato)-ruthenium(II)), and related ligand molecules with a Au(111) surface has been studied using synchrotron radiation-based electron spectroscopy. Resonant photoemission spectroscopy (RPES) and autoionization of the adsorbed molecules have been used to probe the coupling between the molecules and the substrate. Evidence of charge transfer from the states near the Fermi level of the gold substrate into the lowest unoccupied molecular orbital (LUMO) of the molecules is found in the monolayer RPES spectra of both isonicotinic acid and bi-isonicotinic acid (a ligand of N3), but not for the N3 molecule itself. Calibrated x-ray absorption spectroscopy and valence band spectra of the monolayers reveals that the LUMO crosses the Fermi level of the surface in all cases, showing that charge transfer is energetically possible both from and to the molecule. A core-hole clock analysis of the resonant photoemission reveals a charge transfer time of around 4 fs from the LUMO of the N3 dye molecule to the surface. The lack of charge transfer in the opposite direction is understood in terms of the lack of spatial overlap between the π^*-orbitals in the aromatic rings of the bi-isonicotinic acid ligands of N3 and the gold surface. © *2011 American Institute of Physics*. [doi:10.1063/1.3656682]

I. INTRODUCTION

The dye molecule, N3 (cis-bis(isothiocyanato)bis(2,2′-bipyridyl-4,4′-dicarboxylato)-ruthenium(II)) is a photosensitive molecule used in dye-sensitized solar cells (DSCs).[1,2] N3, the structure of which is shown in Figure 1, is one of the most efficient dyes found for DSCs. In these cells, a thin nanocrystalline film of a wide bandgap semiconductor (usually TiO_2) is made sensitive to visible light by a monolayer of dye molecule adsorbed onto the surface. Electrons are promoted from the highest occupied molecular orbital (HOMO) to the lowest unoccupied molecular orbital (LUMO) via excitation from incident light.[1,2] N3 has been shown to bond to TiO_2 via deprotonation of two carboxylic acid groups of its bi-isonicotinic acid ligands forming a 2M-bidentate bond to the surface.[3–5] Bi-isonicotinic acid,[6–9] isonicotinic acid,[10] and related carboxylic acids typically bond to the surface of titanium dioxide via deprotonation of their carboxylic acid groups.[11,12] The chemical coupling allows for the charge transfer of excited electrons from the LUMO of the molecule to the conduction band of the TiO_2.[13,14] This leaves a hole in the HOMO of the molecule which, in a typical DSC, is replenished from an electrolyte.[2] However, an alternative solid state DSC architecture proposed by McFarland and Tang,[15] uses a metal-semiconductor Schottky diode with the dye adsorbed onto an ultrathin metal film on top of the TiO_2 layer. The metal film, which in the case of the original cell was gold, provides a source of electrons to fill the hole in the HOMO. Studying the charge transfer between photosensitive dyes - such as N3 and gold - is, therefore, important to understand this type of DSC architecture.

We have previously reported the adsorption of N3 on gold using scanning tunnelling microscopy and synchrotron-based photoemission.[16] It was found that N3 bonds chemically to the gold surface through one or more of its sulphur atoms and that it adsorbed preferentially at the faulted regions of the Au(111) herringbone reconstruction.[16] Here we present the results from a resonant photoemission spectroscopy (RPES) and x-ray absorption spectroscopy (XAS) study of N3 adsorbed on the Au(111) surface. These techniques allow the electronic structure and the charge transfer interactions between the gold and N3 to be determined by probing the unoccupied levels and the coupling between the surface and the molecule.

When bi-isonicotinic acid[17] and C_{60} (Ref. 18) are each deposited on a gold surface they exhibit distinctive Auger features in the monolayer RPES spectra. It was shown that these features occur due to an Auger decay mechanism termed superspectator decay,[17] where an electron is transferred from the gold surface to the molecule and acts as a spectator for an otherwise normal Auger core-hole decay process. As these features are seen for the bi-isonicotinic acid ligand, the presence of superspectator features in the RPES of the N3 dye molecule is here studied, along with the related molecule, isonicotinic

a)Author to whom correspondence should be addressed. Electronic mail: james.oshea@nottingham.ac.uk.

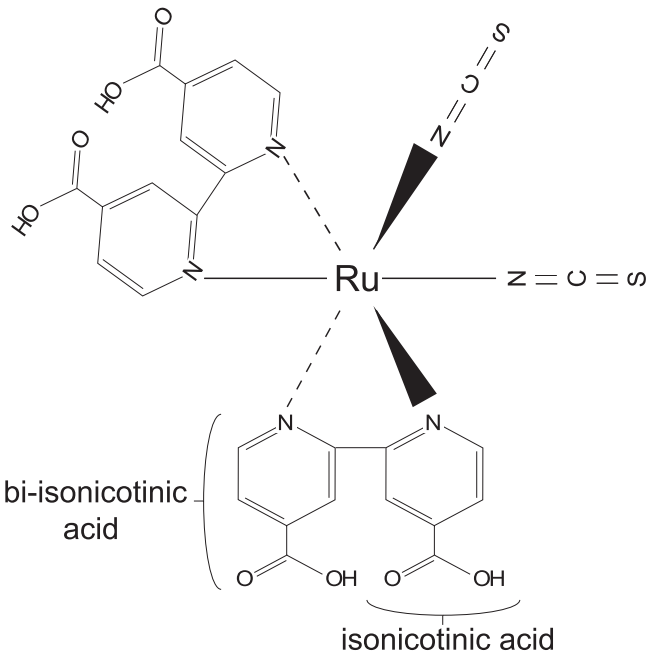

FIG. 1. Schematic representation showing the relationship between the molecular structure of the N3 dye molecule (cis-bis(isothiocyanato)bis(2,2′-bipyridyl-4,4′-dicarboxylato)-ruthenium(II)), the ligand molecule bi-isonicotinic acid (2,2′-bipyridine-4,4′-dicarboxylic acid), and isonicotinic acid (pyridine-4-carboxylic acid).

acid, in order to probe the charge transfer interactions between the N3 dye molecule and the Au(111) surface.

II. METHOD

Experiments were carried out at beamline I311 of the Swedish synchrotron facility MAX-laboratory in Lund.[19] The beamline has a photon energy range of 30–1500 eV and is equipped with a Scienta SES200 hemispherical electron analyzer. The radiation has a high degree of elliptical polarization and may be considered as linearly polarized for the purposes of this study. The base pressure, in the analysis chamber, was in the mid 10^{-11} mbar range and, in the preparation chamber, it was in the low 10^{-10} mbar range.

The substrate was a single crystal of dimensions 10 mm $\times$ 2.5 mm diameter. It was mounted on a loop of tungsten wire (0.5 mm) that passed tightly through the body of the crystal, ensuring a good electrical and thermal contact. A thermocouple was attached within the body of the crystal in order to monitor accurately the temperature. The crystal was cleaned along the lines of Barth *et al.*[20] by cycles of sputtering using 1 kV Ar^+ ions and then annealing at 900 K by passing a current through the tungsten wire mount. Surface contamination was checked by ensuring that the C 1*s*, K 2*p,* and S 2*p* core level photoemission peaks were near or below the detection limits of our measurements.

For the deposition of isonicotinic acid, the molecules were evaporated from a Knudsen cell type evaporator at a temperature of ~10°C onto the sample held at room temperature at a distance of ~20 cm. The bi-isonicotinic acid was also deposited using a Knudsen cell type evaporator, but at the higher temperature of ~230 °C.

In contrast to both isonicotinic acid and bi-isonicotinic acid, N3 undergoes thermal decomposition before it sublimes and therefore cannot be deposited under UHV conditions by thermal evaporation. For this molecule we have used the method of UHV-compatible electrospray deposition, which allows large, fragile, and non-volatile molecules such as N3 to be deposited at close to UHV pressures in coverages ranging from sub-monolayer to multilayer films. This technique has previously been used to study N3 on titanium dioxide[3] and gold surfaces[16] in addition to a wide range of large fragile molecules including single molecule magnets,[21,22] porphyrin nanorings[23] and oligomers,[24] biomolecules,[25] polymers,[26] host-guest complexes,[27] and a range of organometallic dyes.[28,29] The N3 molecule was deposited *in situ* using a commercial UHV electrospray deposition source (Molecularspray, UK) from a solution of ~5 mg of N3 in 200 ml of a 3(methanol):1(water) mixture. The apparatus used and the process by which the molecules are taken from *ex situ* solution to *in situ* vacuum are described in detail elsewhere.[30] Between depositions, the electrospray system was sealed off from the preparation chamber using an UHV gate valve. With the valve open but no electrospray process occurring, the pressure in the preparation chamber was 2×10^{-8} mbar. With the voltage turned on, the preparation chamber pressure rose to 5×10^{-7} mbar, the additional pressure being due to residual solvent molecules in the molecular stream. In all preparations, the coverage was measured using the intensities of the core-level photoemission peaks and the molecule contribution to the shape of the valence band photoemission spectra.

The monochromator exit slits of the beamline were set to give a resolution ~50 meV for photons of energy $h\nu$ = 340 eV. The photon energy was calibrated from the separation between the Au 4*f* peaks measured with 1st and 2nd order radiation. For measuring x-ray absorption and resonant photoemission spectra, a taper was applied to the undulator to reduce the intensity variation of the radiation as the photon energy was scanned. For XAS and RPES measurements, the analyzer pass energy and entrance slits were set to give an analyzer resolution of ~500 meV with respect to binding energy. The analyzer was also set to record spectra in *fixed* mode (where the electron energy window is constant, using the energy dispersion across the detector channels to form the spectrum) for these measurements to give the best compromise between energy resolution and the number of counts required for 2D RPES spectra. For core level photoemission spectra, the analyzer was set to record in *swept* mode (where all detector channels are averaged and the electron energy window is swept through the region of interest) with an overall instrumental resolution of ~100 meV. All three molecules studied suffer beam damage under irradiation by soft x-rays, as characterized previously for bi-isonicotinic acid.[9] In all cases preliminary measurements were performed to determine the exposure limit of the molecules by ensuring that consecutive XPS and XAS spectra were indentical. During the long acquisition times needed for RPES measurements the sample was continuously swept in the beam at a rate of at least 1.25 μm/s.

III. RESULTS AND DISCUSSION

A. Charge transfer from the surface to the molecule

Monolayer and multilayer coverages of bi-isonicotinic acid were deposited on the Au(111) surface by thermal evaporation. The core-level photoemission and x-ray absorption spectroscopy of this surface have been published previously.[17,31] The resonant photoemission spectra for both coverages of bi-isonicotinic acid adsorbed on the Au(111) surface[17,31] are shown in Figure 2. The same spectrum was also measured for the clean Au(111) surface. The two-dimensional RPES datasets were obtained by measuring the valence band photoemission up to 16 eV binding energy for the range of photon energies covering the N 1*s* absorption edge in 0.1 eV steps. The clean surface spectrum (not shown) simply exhibits an intense band due to the direct valence band photoemission of the clean Au(111), as we would expect.

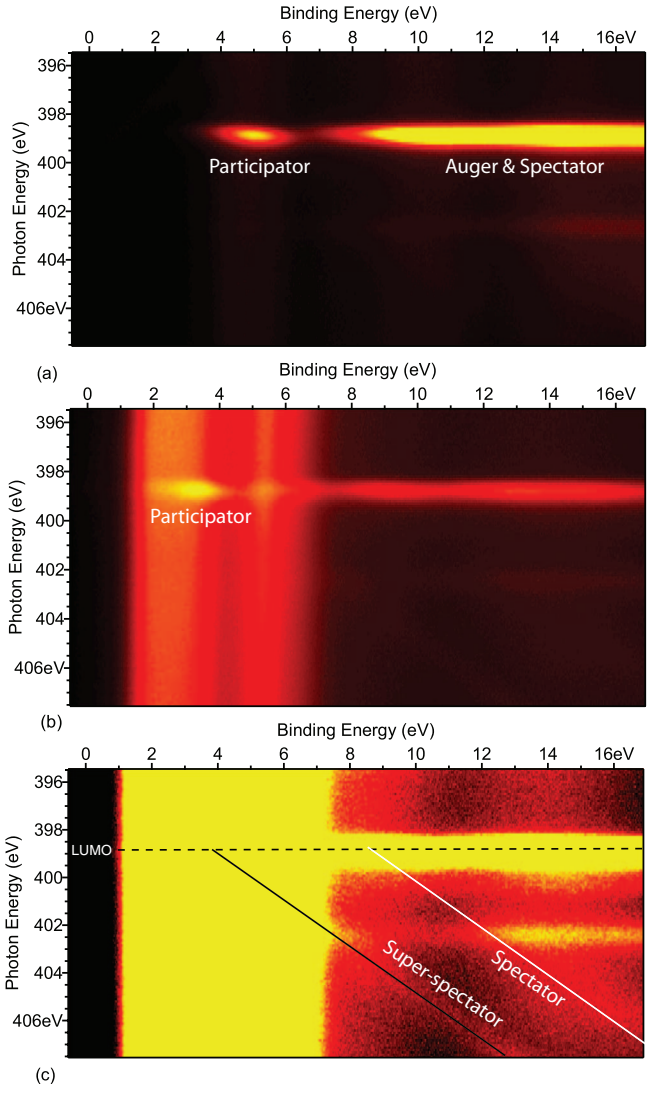

FIG. 2. Resonant photoemission spectra for (a) a multilayer of bi-isonicotinic acid on gold, (b) a monolayer of bi-isonicotinic acid on gold, and (c) the same monolayer spectra as shown in (b) but with the intensity re-scaled to show more clearly the diagonal auger features. The horizontal axis represents the binding energy and the vertical axis the photon energy.

The resonant photoemission spectra for the bi-isonicotinic acid monolayer, shown in Figure 2(b) and with the intensity re-scaled in Figure 2(c), exhibits a number of interesting features. The vertical bands, at low binding energy, are the direct photoemission peaks from the gold surface. The intense band, at a photon energy of 399.8 eV, is due to the excitation of an electron to the LUMO from the core N 1*s* level and the subsequent emission of electrons arising from the decay of the core-hole produced. Superimposed on the gold direct photoemission peaks at low binding energy, there is *participator decay* at the LUMO resonance. *Participator decay* is the process which occurs due to the originally excited electron (in this case to the LUMO) being involved in the non-radiative decay of the N 1*s* core-hole. This leads to a final state identical to that of direct photoemission, as shown in Figure 3(b), and is clearly visible as a strong enhancement at 5 eV binding energy in the multilayer spectrum in Figure 2(a) and 3.5 eV in the monolayer spectrum in Figure 2(b).

As well as participator electrons, there are also constant kinetic energy features which result from *spectator decay* of the core-hole. They arise from the originally excited electron not being involved in the decay process, except as a spectator, during a normal Auger decay process in which the N 1*s* core-hole is filled instead by another valence electron. The spectator electron induces a small upward shift in energy due to its presence in the unoccupied state (Figure 3(c)). These spectator electrons, along with normal Auger electrons, account for the high intensity region observed in the RPES spectra on the right-hand side drifting linearly out of the binding energy window due to their constant kinetic energy.

The monolayer RPES spectrum of bi-isonicotinic acid on gold (Figure 2(c)) shows an interesting diagonal Auger feature that is not observed for the multilayer or the clean surface spectra. Such features were also observed recently for a C_{60} monolayer on gold,[18] and attributed to spectator decay following charge transfer from the surface to the

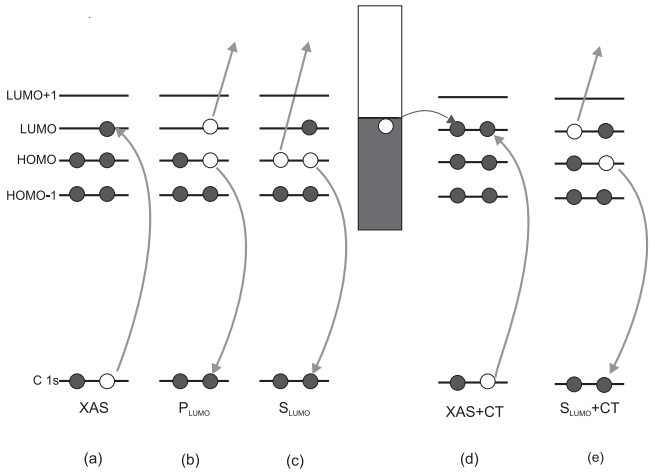

FIG. 3. Electron excitation and de-excitation processes: (a) Resonant core level excitation into unoccupied bound states (x-ray absorption); (b) Participator decay following x-ray absorption induced core-hole; (c) Spectator core-hole decay; (d) X-ray absorption in the presence of charge transfer from states near the Fermi level of the metal substrate; and (e) spectator core-hole decay in the presence of charge transfer.

molecule, as depicted in Figure 3(e). As in the case of spectator Auger electrons, the energy of electrons emitted in this process have a constant kinetic energy and therefore disperse linearly through the RPES binding energy window as the photon energy is increased. What differentiates this so-called superspectator channel from that of spectator is the upward shift in kinetic energy. In a spectator decay, the emitted electron originates from the HOMO level as depicted in Figure 3(c), however, in superspectator decay the emitted electron originates from the LUMO, and is therefore shifted up in energy by an amount corresponding to the HOMO-LUMO gap of the molecule. Since this energy is typically a few eV for most molecules, the constant kinetic energy feature associated with this charge-transfer Auger process is easily resolved from the spectator channel. The presence of these so-called superspectator lines in a RPES spectrum is therefore indicative of surface-to-molecule charge transfer.

The corresponding isonicotinic acid monolayer RPES spectrum looks almost identical to that of bi-isonicotinic acid, as shown in Figure 4(c). The charge transfer Auger feature is observed as a diagonal line of higher intensity from a binding energy of 9 eV at 403 eV photon energy to a binding energy of 15 eV at 409 eV photon energy. This is highlighted by a the superimposed solid black line. This feature actually tracks back to the LUMO photon energy at a binding energy of around 4 eV, the position of the HOMO-LUMO participator peak.

Monolayer and multilayer coverages of N3 were deposited on the Au(111) surface by *in situ* electrospray deposition. The core-level and valence photoemission measured were found to be consistent with those previously published for N3 adsorbed on Au(111).[16] The N3 monolayer RPES shown in Figure 5(b) presents a very different picture. The spectrum closely resembles the N3 multilayer RPES, except that the gold photoemission peaks are much more pronounced and the molecule's LUMO resonance have a much lower intensity. What is most surprising is that the monolayer spectrum, even when the intensity has been re-scaled as in Figure 5(c), lacks the diagonal Auger feature observed in the monolayer RPES spectra of the other two molecules adsorbed on the Au(111) surface. This data suggests that while charge transfer from the surface to the bi-isonicotinic acid ligands of N3 does not occur when they are bound within the dye complex.

Charge transfer between the molecule and the substrate, in either direction, depends on the energetics of the lowest unoccupied molecular orbitals with respect to the substrate density of states. If the LUMO lies below the Fermi level of the gold surface, then charge transfer is possible from the surface to the adsorbed molecules. In the core-excited state, the presence of the core-hole can lead to the LUMO state being excitonically pulled down so that it crosses the Fermi level of the gold surface.[32] We can measure the position of the core-excited LUMO of each molecule, with respect to the Fermi level, by placing the calibrated N 1*s* XAS and valence band photoemission for each monolayer on a common binding energy scale,[33] as shown in Figure 6. The data shows that the LUMO of all the molecules lies mostly below the Fermi level of the Au(111) surface in the core-excited state. This would

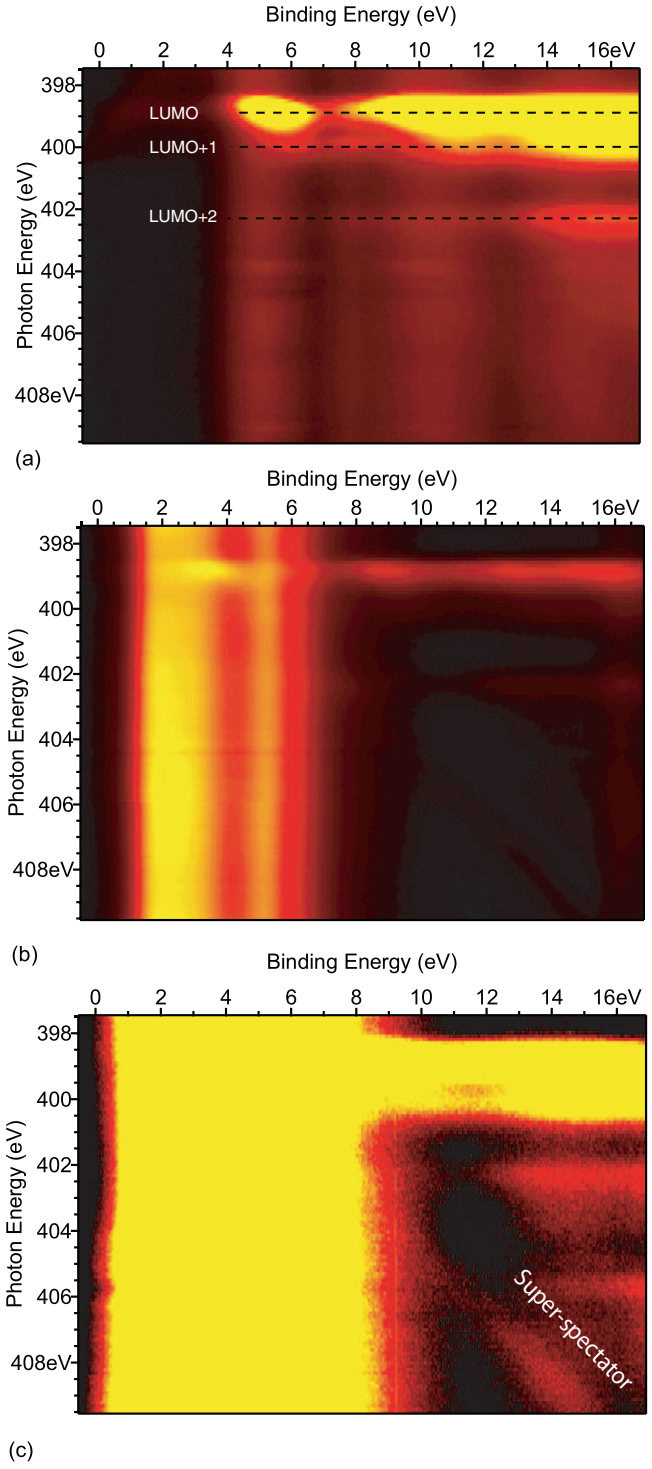

FIG. 4. Resonant photoemission spectra for (a) a multilayer of isonicotinic acid on gold, (b) a monolayer of isonicotinic acid on gold, and (c) the same monolayer spectra as shown in (b) but with the intensity re-scaled to show more clearly the diagonal auger features.

theoretically allow the transfer of electrons from the valence band of the metal to the majority of the vibronic states of the core-excited LUMO that now lie below the Fermi level of the gold surface. However, energetic overlap is a necessary but not sufficient condition for charge transfer to occur as illustrated in the case of N3. Spatial overlap of the molecular orbitals involved is also required, and the difference in

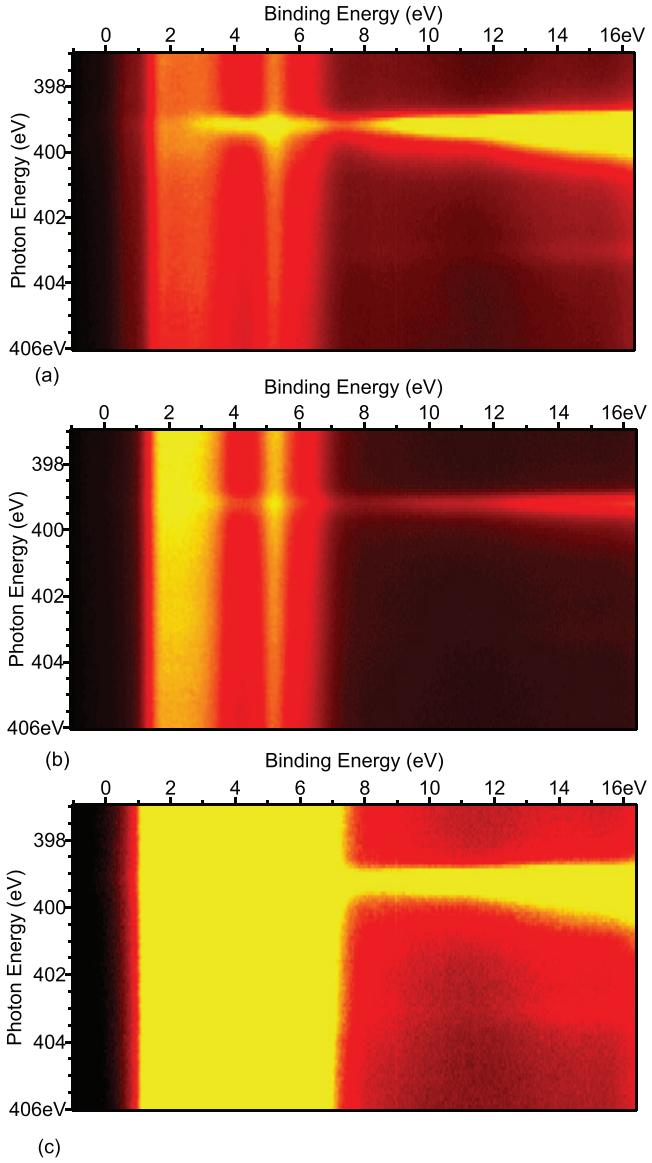

FIG. 5. Resonant photoemission spectra for (a) a multilayer of N3 on gold, (b) a monolayer of N3 on gold, and (c) the same monolayer spectra as shown in (b) but with the intensity re-scaled like in Figures 2 and 4, showing a clear absence of any diagonal auger features.

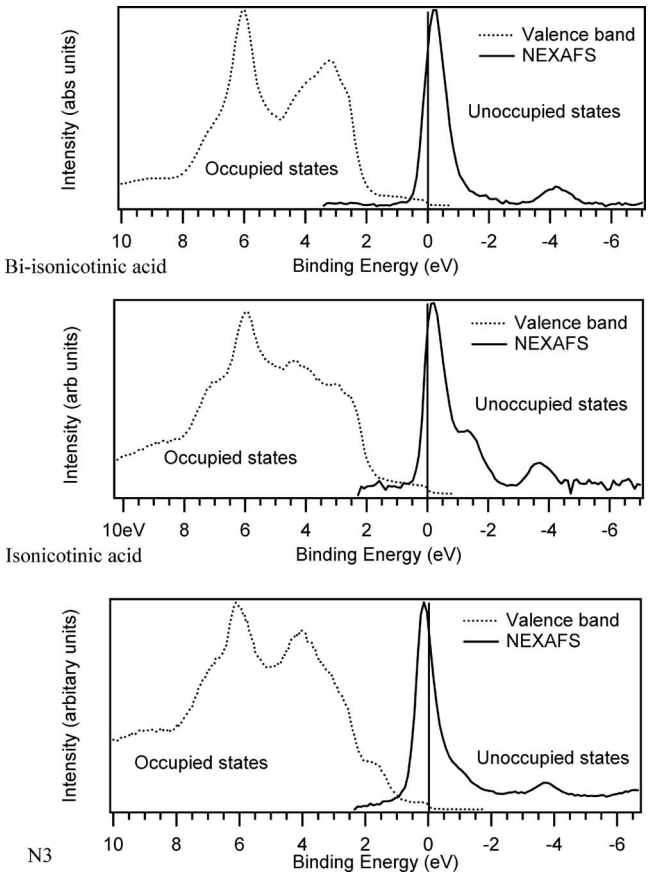

FIG. 6. Energy level alignment of the substrate valence band and the unoccupied molecular orbitals of the molecule for bi-isonicotinic acid (top), isonicotinic acid (middle), and N3 (bottom). All spectra have been calibrated to the Fermi edge of the gold surface at 0 eV binding energy.

behaviour of N3 compared to its ligand molecules is therefore most likely associated with its adsorption geometry on the surface.

Previous results have shown that the N3 molecule chemically bonds to the gold surface mostly through one or more sulphur atoms of the thiocyanate ligands.[3] As in the case of bi-isonicotinic acid molecules on Au(111), no deprotonation of the carboxylic acid groups occurs, suggesting a largely van der Waals interaction between these ligands and the surface. This does not preclude charge transfer as demonstrated for bi-isonicotinic acid itself. However, the largely octahedral geometry of the molecule prevents the bi-isonicotinic acid ligands from lying flat on the surface in any orientation, as illustrated in Figure 7. This means that the π-orbitals of the pyridine rings of these ligands have little or no spatial overlap with the dangling 5*d* orbitals of the gold surface. This is important as density functional theory calculations show that the LUMO is predominantly derived from the π-orbitals of the pyridine rings.[3] Electrons therefore cannot tunnel easily from the surface to the LUMO of the molecule. Charge transfer can occur for bi-isonicotinic acid on gold because the molecule lies flat on the surface[17] allowing for the overlap between the orbitals and, therefore, there can be a high degree of spatial overlap

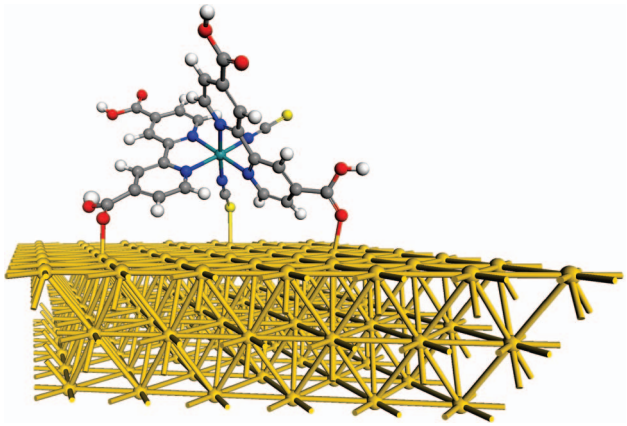

FIG. 7. Schematic molecular model of one possible configuration of the N3 molecule on the Au(111) surface. Even though in this case the bi-isonicotinic acid ligands are in contact with the surface, the octahedral geometry of the molecule prevents them from lying flat on the surface in all orientations.

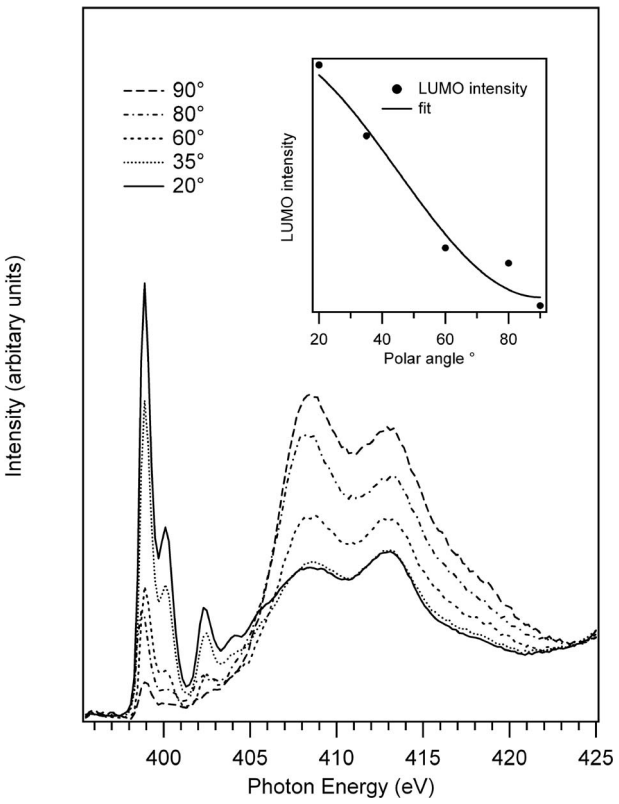

FIG. 8. Angle resolved XAS spectra for a monolayer of isonicotinic acid adsorbed on the Au(111) surface. Inset shows the variation of the LUMO intensity with the angle of the incident radiation to the surface normal. The fit curve is the theoretical angular dependence for an aromatic ring with tilt angle of 89 ± 1° to the surface normal, assuming a random azimuthal orientation and linear light polarization (see Refs. 34 and 35).

between the π-orbitals and the dangling 5*d* orbitals of the gold surface.

The adsorption geometry of isonicotinic acid molecules on the Au(111) surface has here been studied using angle resolved XAS. The data in Figure 8 shows the spectra measured over the N 1*s* edge, for a range of angles. The spectra have been corrected for undulator intensity variations and normalized to the continuum of states above the vacuum level (425 eV).[6,8] The angles quoted are those between the surface normal and the electric field vector of the incoming radiation. Only polar angles were considered as the substrate has a 6-fold rotational symmetry, eliminating azimuthal intensity variations.[34,35] The sharp low energy peaks below 406 eV are identified with the π^* unoccupied molecular orbitals, associated with the planar aromatic ring of the molecule.[12] Maximal π^* intensity is observed to occur for the electric field perpendicular to the plane of the surface, with minimal intensity for the field oriented in the parallel direction. An analysis of the LUMO intensity variation as a function of angle,[34,35] reveals that the plane of the aromatic ring structure has an average tilt angle of 89° ± 1° to the surface normal. Isonicotinic acid therefore adsorbs parallel to the metal surface which maximizes the electronic coupling, allowing charge transfer from the surface to the molecule as discussed in the case of bi-isonicotinic acid. Configuration dependent charge transfer has previously been observed for the planar aromatic molecule 4-fluorobenzenethiol on the Au(111) surface,[36] although in that case it was charge transfer from the molecule to the surface under investigation.

B. Charge transfer from the molecule to the surface

The absence of any charge-transfer Auger-decay features in the N3 monolayer RPES would imply that there is no charge transfer *from* the metal *to* the N3 molecule, unlike for bi-isonicotinic acid and isonicotinic acid. But this does not preclude charge transfer in the opposite direction. An electron transfer from the continuum of states of the metal surface into a discrete molecular state requires both a strong electronic coupling and nuclear relaxation. An electron making the transition from a discrete molecular state into the continuum of conduction band states will delocalize, existing in a mixed state where it will coherently sample all coupled states, breaking the resonance with the electronic state on the molecule on the femtosecond time scale and localizing the electron within the substrate.[37] We can get a measure of the charge transfer dynamics from the molecule to the gold surface by using the *core-hole clock* implementation of RPES. This method is based on the principle that the participator core-hole decay channel (Figure 3(b)) requires localization of the core-excited electron in the probed unoccupied state on the time scale of the core-hole lifetime. The absence of participator electrons in resonant photoemission is therefore indicative of ultra-fast charge transfer.[38]

An integration of the participator electron intensity over the HOMO and HOMO-1 of N3 (1–7 eV) as a function of photon energy is shown for both the multilayer and monolayer in Figure 9, and compared to the associated x-ray absorption spectrum (normalized in this case to the intensity of the LUMO+1 for the reasons explained below). A large

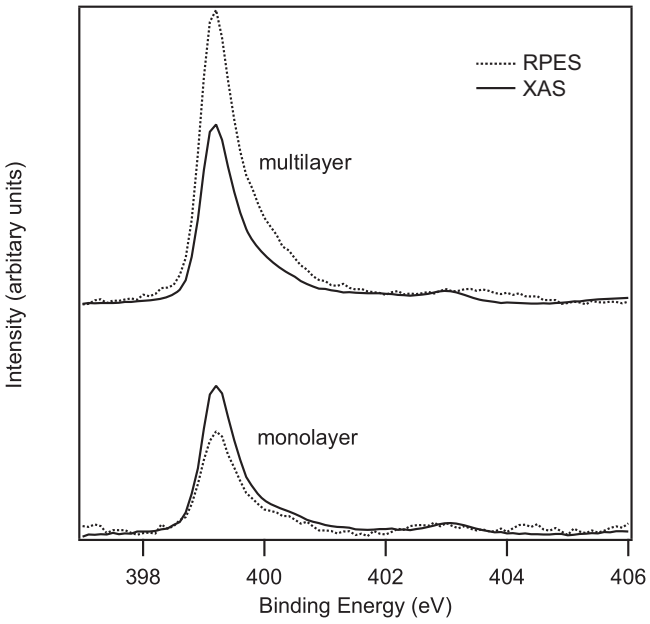

FIG. 9. N 1*s* RPES and N 1*s* XAS spectra of the N3 multilayer and monolayer on Au(111). The RPES spectra, shown here, are binding energy integrations from 1 to 7 eV for the datasets shown in Figure 5. The spectra have been normalized to the LUMO+2 at 402.5 eV.

proportion of participator electrons is expected in the case of the multilayer because the molecules are effectively isolated from the substrate which means that no charge transfer can take place. Electrons excited to the LUMO, LUMO+1, and LUMO+2, therefore, remain on the molecule long enough to participate in the core-hole decay, leading to a final state identical to direct photoemission of the HOMO state involved (Figure 3(b)). In fact, the multilayer is taken as the benchmark in the core-hole clock analysis to determine the anticipated participator intensity for each LUMO state in the absence of charge transfer.[3,14,38]

Unfortunately, in this case, the core-hole clock analysis used for molecules adsorbed on wide bandgap semiconductor surfaces,[3,13,14,39] such as TiO_2 (in which the LUMO lies entirely within the bandgap) is unsuited to give us an exact quantitative picture of the transfer from either bi-isonicotinic acid, isonicotinic acid or the N3 dye molecule adsorbed on Au(111). This is due to the fact that, as the LUMO of all the molecules in the core-excited state lies both partially above and below the Fermi level of the gold substrate, charge transfer can occur from those vibronic states of the LUMO that lie above the Fermi level of the substrate, rendering normalization to the LUMO inappropriate. However, an upper limit for the charge transfer time out of the LUMO into the gold surface can be obtained by making two assumptions.

The first assumption is that there is no charge transfer from the LUMO+2 (between 402 and 403 eV for our molecules) to the surface. This allows for normalization to the LUMO+2 in order to analyse the changes in the intensity of the LUMO itself. It must be stressed that this assumption need not be true in order to provide us with an upper limit for electron transfer from the LUMO. Any charge transfer out of this state ignored in our analysis simply leads to an underestimate of the true participator intensity for this state, which in turn leads to an overestimate of participator intensity at the LUMO, serving only to lengthen the calculated charge transfer time.

The second assumption is that there is no charge transfer from the surface into those vibronic states of the LUMO that lie below the Fermi level. We already know from the data presented in Sec. III A that in the case of bi-isonicotinic acid and isonicotinic acid, this assumption is certainly not valid. The presence of the diagonal superspectator features observed in Figures 2 and 4 are indicative of precisely this charge transfer into the LUMO. For this reason, the following analysis cannot be used at this time for the bi-iso and iso molecules (at least not until we can quantify the amount of charge transfer into the LUMO). However, the assumption is valid for N3 since the data in Sec. III A shows that there is no charge transfer from the surface to the N3 molecule and thus any decrease in the LUMO participator intensity can be entirely attributed to charge transfer from the LUMO to the gold surface.

Denoting the intensity of the LUMO as I, the average electron injection time, τ_{El}, for electrons moving from the LUMO to unoccupied substrate states is determined from Eq. (1),

$$\tau_{El} = \tau_{CH} \frac{I^{mono}_{RPES}/I^{mono}_{XAS}}{I^{multi}_{RPES}/I^{multi}_{XAS} - I^{mono}_{RPES}/I^{mono}_{XAS}}. \quad (1)$$

A more thorough discussion of the core-hole clock implementation of RPES and a derivation of the equation is given by Brühwiler *et al.*[38] I^{mono}_{RPES} and I^{multi}_{RPES} represent the intensities of the LUMO peaks in the RPES monolayer and multilayer, respectively. They are normalized by the XAS intensities, I^{mono}_{XAS} and I^{multi}_{XAS}. τ_{CH} is the average lifetime of an N 1*s* core-hole that has been measured to be 6 fs.[40] For the N3 on gold core-hole clock analysis, $I^{mono}_{RPES}/I^{mono}_{XAS} = 0.69$ and $I^{multi}_{RPES}/I^{multi}_{XAS} = 1.64$, giving an overall upper limit for the charge injection time of 4.4 fs from the LUMO to the conduction band of the surface.

IV. CONCLUSION

The RPES spectra of an N3 monolayer on gold do not exhibit the *superspectator* features observed for the monolayer RPES spectra of other molecules such as bi-isonicotinic acid, isonicotinic acid, and C_{60}. This is surprising as bi-isonicotinic acid is a ligand of N3 and would thus be expected to share similar characteristics. These features are due to the Auger decay of an electron from the LUMO being spectated by an electron transferred from the surface to the molecule. The lack of such a decay channel in N3 suggests that there is almost no charge transfer from the gold surface into the N3 molecule. By placing the XAS and valence band photoemission on a common binding energy scale, the LUMO of the N3 molecule is revealed to lie partially below the Fermi edge of the gold metal, showing that it is energetically possible for charge transfer to occur in the core-excited state. The reason for the lack of charge transfer from the gold surface to the N3 molecules is attributed to the geometry of the molecule on the surface as the π^*-orbitals of the aromatic rings in the bi-isonicotinic acid ligands (which have been shown to contain the LUMO orbitals) lack the required spatial overlap with the 5*d* orbitals of the gold surface. This significantly reduces the chances of an electron tunnelling from the surface to the molecule. On the other hand, charge *from* the LUMO of the molecule to the substrate conduction band does occur in the case of N3, for which the core-hole clock implementation of RPES places an upper limit on the time scale of this process at 4.4 fs.

ACKNOWLEDGMENTS

The authors are grateful for financial support by the European Community Research Infrastructure Action under the FP6 Structuring the European Research Area Programme (through the Integrated Infrastructure Initiative Integrating Activity on Synchrotron and Free Electron Laser Science), and the UK Engineering and Physical Sciences Research Council (EPSRC).

[1] B. O'Regan and M. Grätzel, Nature (London) **335**, 737 (1991).
[2] M. Grätzel, J. Photochem. Photobiol. C **4**, 145 (2003).
[3] L. C. Mayor, J. B. Taylor, G. Magnano, A. Rienzo, C. J. Satterley, J. N. O'Shea, and J. Schnadt, J. Chem. Phys. **129**, 114701 (2008).
[4] H. Rensmo, S. Södergren, L. Patthey, K. Westermark, L. Vayssieres, O. Kohle, P. Brühwiler, A. Hagfeldt, and H. Siegbahn, Chem. Phys. Lett. **274**, 51 (1997).

[5]E. M. J. Johansson, M. Hedlund, H. Siegbahn, and H. Rensmo, J. Phys. Chem. B **109**, 22256 (2005).
[6]L. Patthey, H. Rensmo, P. Persson, K. Westermark, L. Vayssieres, A. Stashans, Å. Petersson, P. A. Brühwiler, H. Siegbahn, S. Lunell, and N. Mårtensson, J. Chem. Phys. **110**, 5913 (1999).
[7]A. Thomas, W. Flavell, C. Chatwin, S. Rayner, D. Tsoutsou, A. Kumarasinghe, D. Brete, T. Johal, S. Patel, and J. Purton, Surf. Sci. **592**, 159 (2005).
[8]P. Persson, S. Lunell, P. A. Brühwiler, J. Schnadt, S. Södergren, J. N. O'Shea, O. Karis, H. Siegbahn, N. Mårtensson, M. Bässler, and L. Patthey, J. Chem. Phys. **112**, 3945 (2000).
[9]J. N. O'Shea, J. B. Taylor, L. C. Mayor, J. C. Swarbrick, and J. Schnadt, Surf. Sci. **602**, 1693 (2008).
[10]J. N. O'Shea, J. Schnadt, P. A. Brühwiler, H. H. N. Mårtensson, L. Patthey, J. Krempaský, C. Wang, Y. Luo, and H. Ågren, J. Phys. Chem. B. **105**, 1917 (2001).
[11]J. Schnadt, J. N. O'Shea, L. Patthey, J. Schiessling, J. Krempaský, M. Shi, N. Mårtensson, and P. A. Brühwiler, Surf. Sci. **544**, 74 (2003).
[12]J. Schnadt, J. Schiessling, J. N. O'Shea, S. M. Gray, L. Patthey, M. K. J. Johansson, M. Shi, J. Krempaský, J. Åhlund, P. G. Karlsson, P. Persson, N. Mårtensson, and P. A. Brühwiler, Surf. Sci. **540**, 39 (2003).
[13]J. Schnadt, J. O'Shea, L. Patthey, L. Kjeldgaard, J. Ahlund, K. Nilson, J. Schiessling, J. Krempasky, M. Shi, O. Karis, C. Glover, H. Siegbahn, N. Martensson, and P. Bruhwiler, J. Chem. Phys. **119**(23), 12462 (2003).
[14]J. Schnadt, P. A. Brühwiler, L. Patthey, J. N. O'Shea, S. Södergren, M. Odelius, R. Ahuja, O. Karis, M. Bässler, P. Persson, H. Siegbahn, S. Lunell, and N. Mårtensson, Nature (London) **418**, 620 (2002).
[15]E. W. McFarland and J. Tang, Nature (London) **421**, 616 (2003).
[16]L. C. Mayor, A. Saywell, G. Magnano, C. J. Satterley, J. N. OShea, and J. Schnadt, J. Chem. Phys. **130**, 164704 (2009).
[17]J. B. Taylor, L. C. Mayor, J. C. Swarbrick, and J. O'Shea, J. Chem. Phys. **127**, 134707 (2007).
[18]A. J. Britton, A. Rienzo, K. Schulte, and J. N. O'Shea, J. Chem. Phys. **133**, 094705 (2010).
[19]R. Nyholm, J. N. Andersen, U. Johansson, B. N. Jensen, and I. Lindau, Nucl. Instrum. Methods Phys. Res. B **467–468**, 520 (2001).
[20]J. V. Barth, H. Brune, G. Ertl, and R. J. Behm, Nucl. Instrum. Meth. B **42**, 9307 (1990).
[21]A. Saywell, A. J. Britton, N. Taleb, M. D. Giménez-López, N. R. Champness, P. H. Beton, and J. N. O'Shea, Nanotechnology **22**, 075704 (2011).
[22]A. Saywell, G. Magnano, C. J. Satterley, L. M. A. Perdigão, A. J. Britton, N. Taleb, M. D. Giménez-López, N. R. Champness, J. N. O'Shea, and P. H. Beton, Nat. Commun. **1**, 75 (2010).
[23]M. C. O'Sullivan, J. K. Sprafke, D. V. Kondratuk, C. Rinfray, T. D. W. Claridge, A. Saywell, M. O. Blunt, J. N. O'Shea, P. H. Beton, M. Malfois, and H. L. Anderson, Nature (London) **469**(7328), 72 (2011).
[24]A. Saywell, J. K. Sprafke, L. J. Esdaile, A. J. Britton, A. Rienzo, H. L. Anderson, J. N. O'Shea, and P. H. Beton, Angew. Chem., Int. Ed. **49**, 9136 (2010).
[25]S. Rauschenbach, F. L. Stadler, E. Lunedei, N. Malinowski, S. Koltsov, G. Costantini, and K. Kern, Small **2**, 540 (2006).
[26]J. E. Lyon, A. J. Cascio, M. M. Beerborn, R. Schlaf, Y. Zhu, and S. A. Jenekhe, Appl. Phys. Lett. **88**, 222109 (2006).
[27]N. Thontasen, G. Levita, N. Malinowski, Z. Deng, S. Rauschenbach, and K. Kern, J. Phys. Chem. C **114**, 17768 (2010).
[28]M. Weston, A. J. Britton, and J. N. O'Shea, J. Chem. Phys. **134**, 054705 (2011).
[29]M. Weston, T. J. Reade, A. J. Britton, K. Handrup, N. R. Champness, and J. N. O'Shea, J. Chem. Phys. **135**, 114703 (2011).
[30]C. J. Satterley, L. M. A. Perdigäo, A. Saywell, G. Magnamo, A. Rienzo, L. C. Mayor, V. R. Dhanak, P. H. Beton, and J. N. OShea, Nanotechnology **18**, 455304 (2007).
[31]J. B. Taylor, L. C. Mayor, J. C. Swarbrick, J. N. OShea, and J. Schnadt, J. Phys. Chem. B **111**, 16646 (2007).
[32]J. Schnadt, J. Schiessling, and P. A. Brühwiler, Chem. Phys. **312**, 39 (2005).
[33]J. Schnadt, J. N. OShea, L. Patthey, J. Krempasky, N. Mårtensson, and P. A. Brühwiler, Phys. Rev. B **67**, 235420 (2003).
[34]J. Stöhr, *NEXAFS Spectroscopy* (Springer, Berlin, 1992).
[35]J. Stöhr and D. A. Outka, Phys. Rev. B **36**, 7891 (1987).
[36]L. Wang, L. Liu, W. Chen, Y. Feng, and A. T. S. Wee, J. Am. Chem. Soc. **128**(24), 8003 (2006).
[37]J. M. Lanzafame, R. J. D. Miller, A. A. Muenter, and B. A. Parkinson, J. Phys. Chem. **96**(7), 2820 (1992).
[38]P. A. Brühwiler, O. Karis, and N. Mårtensson, Rev. Mod. Phys. **74**, 703 (2002).
[39]M. Weston, A. J. Britton, and J. N. O'Shea, J. Chem. Phys. **134**(5), 054705 (2011).
[40]B. Kempgens, A. Kivimäki, M. Neeb, H. M. Köppe, A. M. Bradshaw, and J. Feldhaus, J. Phys. B - At. Mol. Opt. **29**, 5389 (1996).